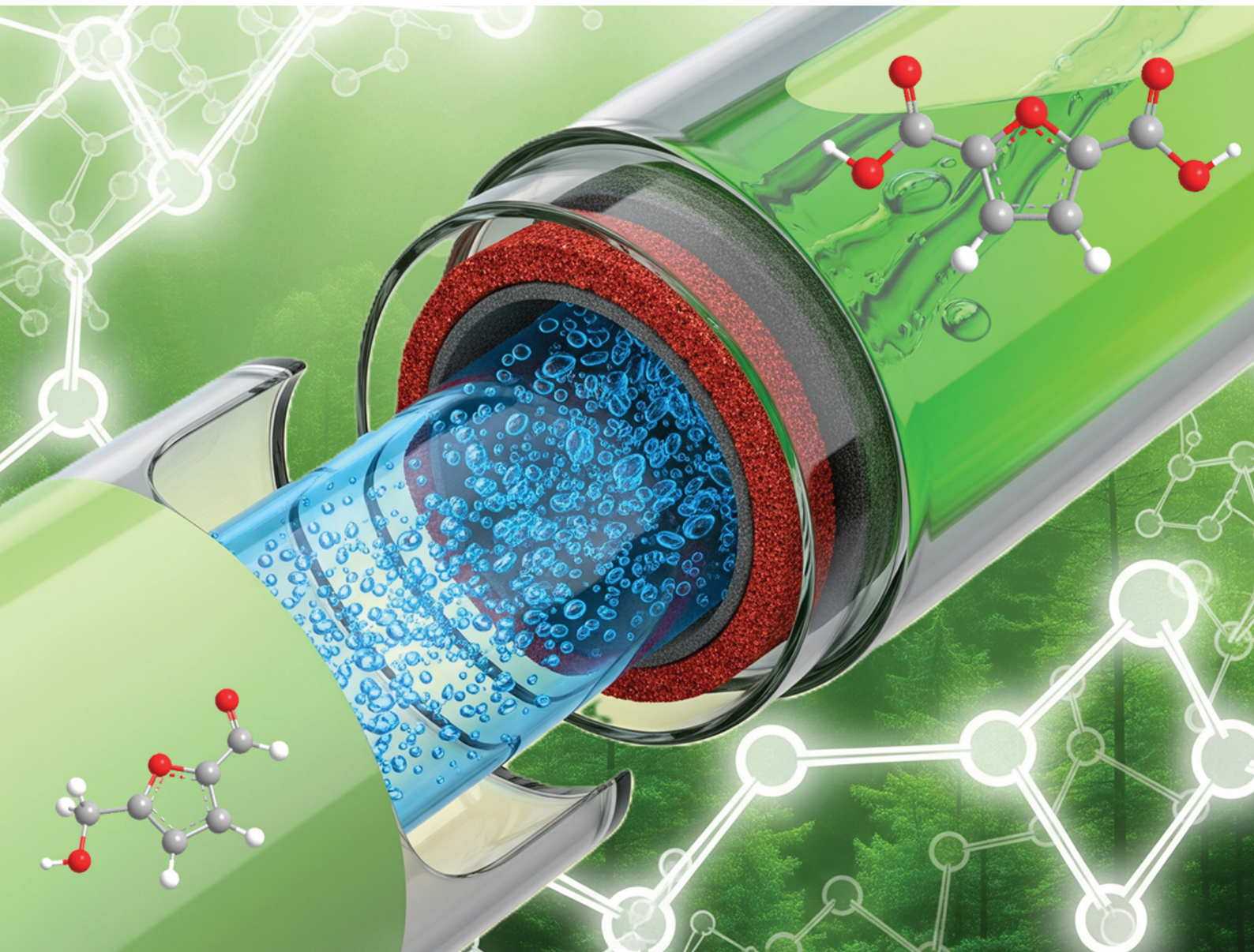


Green Chemistry

Cutting-edge research for a greener sustainable future

rsc.li/greenchem



ISSN 1463-9262

PAPER

Luigi Vaccaro *et al.*

Continuous flow tube-in-tube oxidation of HMF to FDCA using heterogeneous manganese catalyst under mild conditions



Cite this: *Green Chem.*, 2025, **27**, 12166

Continuous flow tube-in-tube oxidation of HMF to FDCA using heterogeneous manganese catalyst under mild conditions[†]

Federica Valentini,[‡] Francesco Ferlin [‡] and Luigi Vaccaro ^{*}

The shift from a petrol-based to a bio-based society and economy is already underway. Continuous development is required to seek increasingly efficient methodologies capable of being competitive with the current production chain. 2,5-furan dicarboxylic acid (FDCA) currently represents, together with its precursor 5-hydroxymethylfurfural (HMF), among the major players in the sector of products derived from biomass due to their potential use as building blocks for the synthesis of bio-plastics or bio-polymers in general. Among the many methods reported for the selective oxidation of HMF to FDCA, the use of heterogeneous catalysts based on noble metals is widely studied. However, these catalysts represent a problem in terms of resource scarcity and are often synthesised using complex procedures. In addition, most systems for the oxidation of HMF to FDCA make use of oxygen at high pressures and high reaction temperatures. In this contribution, we report our efforts to develop a continuous flow apparatus for the selective oxidation of HMF to FDCA using an easy-to-synthesize manganese-based catalyst. By sequentially evaluating the design, construction, and use of different flow systems, we finally were able to propose a system that allowed the use of the manganese catalyst at relatively low temperatures and pressures, comparable to or even better than those utilised for noble-metal catalysts, with excellent efficiency and productivity.

Received 17th May 2025,
Accepted 1st June 2025

DOI: 10.1039/d5gc02459e
rsc.li/greenchem



Green foundation

1. The work implements the utilization of tube-in-tube continuous flow technology for the selective synthesis of FDCA from HMF proving that within this approach it is possible to utilize simple Mn-based catalyst in mild conditions with competitive results compared to Noble Metal based catalysts.
2. Calculation of the green metric (*E*-factor), of safety parameter (RTHI, RPHI) and Space-TimeYield, together with a newly defined Oxygen efficiency for the process in exam and for literature protocols also prove the advancement in overall sustainability.
3. The inherent safety and convenience in using Air as cheap terminal oxidant allows for continuous synthesis of FDCA with a low *E*-factor and an impressive STY.

Introduction

Valorisation of renewable and biodegradable feedstock to produce value-added chemicals and fuels appears as one of the possible and interesting routes to finding an alternative to the petrol-based industry.^{1,2} Attention to bio-based industry is currently boosting as both businesses and consumers are

looking for safer and cheaper access to bio-based platform chemicals and commodities.³

Biomass can be an easily accessible and inexpensive raw material with a pivotal role in global carbon balance and CO₂ compensation.⁴ In the last decade, numerous research studies have been concentrated on finding specific uses for the various platform chemicals deriving from the valorisation of biomass from biorefineries,⁵ using an approach somewhat similar to what was done in the last century with petrol refineries.⁶

Among the many platform chemicals identified for sustainable chemical production, 5-hydroxymethylfurfural (HMF) has been recognised as one of the most strategic products derived from carbohydrate dehydration.⁷ Also known as “the sleeping giant”, HMF is currently listed in the top 12 chemicals (US

Laboratory of Green S.O.C. – Dipartimento di Chimica, Biologia e Biotecnologie,
Università degli Studi di Perugia, Via Elce di Sotto 8, 06123 – Perugia, Italy.

E-mail: luigi.vaccaro@unipg.it; <https://greensoc.chm.unipg.it>

[†] Electronic supplementary information (ESI) available: General procedures, full characterization of the synthesized compounds and copies of ¹H, ¹³C and ¹⁹F NMR spectra. See DOI: <https://doi.org/10.1039/d5gc02459e>

[‡] These authors have contributed equally to this work.

DOE) that can be produced from bio-renewable resources due to its many industrial application and to its many interesting derivatives.⁸

In fact, HMF can be transformed into other platform chemicals such as γ -valerolactone and levulinic acid or,⁹ by oxidation, to 2,5-diformylfuran (DFF), 5-hydroxymethyl-2-furancarboxylic acid (HMFCA), 5-formyl-2-furancarboxylic acid (FFCA), 2,5-furandicarboxylic acid (FDCA).¹⁰

FDCA, owing two carboxylic functionalities, is a terephthalic acid mimic and, therefore, is a solid, promising constituent of green polymers such as poly(ethylene 2,5-furan dicarboxylate) (PEF).¹¹

Due to this peculiarity, FDCA has gained enormous interest with the hope of replacing high-volume petroleum-based building blocks for polymer production.¹²

Oxidation of HMF to FDCA lies into a consecutive oxidation pathway in which HMF is firstly oxidised to either 5-hydroxymethylfurfural-carboxylic acid (HMFCA) or 2,5-diformylfuran (DFF). These intermediates are then subsequently oxidised to 5-formylfuran-2-carboxylic acid (FFCA) and finally to FDCA.¹³

To date, a plethora of conventional and unconventional methodologies and catalysts have been employed to investigate the oxidation of HMF to FDCA.¹⁴ The intrinsic reactivity of HMF represents an essential difficulty in controlling the selectivity of this process. In fact, the concomitant presence of a furan ring, a formyl functionality and a hydroxyl group renders HMF highly susceptible to many side reactions.¹⁵ In general, byproducts derived from HMF are the major limitation on the route towards the efficient synthesis of FDCA.

Two major byproducts have generally been encountered: (i) humins formed especially at high temperatures and in the presence of strongly basic conditions, and (ii) levulinic acid formed *via* rehydration of HMF in aqueous reaction media.¹⁶

The oxidation of HMF to FDCA is a transformation of great interest to sustainability. To optimise such a process, it is also necessary to consider the factors that may influence the overall environmental benignity and economic impact of the process, such as the catalyst, the type of oxidant, and the solvent/medium selection for performing and isolating the desired FDCA.

The use of heterogeneous catalysis for HMF oxidation is arguably the elected choice nowadays, proved that the possible advantages are achieved, as the easier recovery, reuse, and minimal product contamination. At the same time, most of the catalysts are based on precious noble metals, leading to a significant impact in terms of resource depletion and production cost.¹⁷ Many studies highlighted how the performance of heterogeneous catalysts in HMF oxidation is highly dependent on the geometry and acid/basic nature of their active sites.¹⁸ Indeed, deactivation is not only a consequence of leaching or coalescence under harsh conditions but also depends on the irreversible adsorption of humins onto the catalyst surface.¹⁹

Besides the low stability of HMF in water, water is the most used reaction medium as it is cheap and more environmentally friendly than dipolar aprotic solvents DMSO and DMF,

which are also often used as alternatives. Moreover, water can favour the work-up procedures, letting FDCA precipitate by simply changing the pH of the final reaction mixture.

Proper selection of the oxidant system, which is the subject of extensive research, is of outmost importance.^{10^e,20} Chemical oxidants not only increase the total mass of reactants, generating a larger amount of waste, but they also complicate the final reaction mixture composition with a consequently additional wasteful and tedious product isolation. Gaseous oxidants, on the other hand, can be difficult or hazardous to manipulate, especially at high pressure.

Coherently to our research approach,²¹ we have decided to investigate the oxidation of HMF to FDCA trying to identify a protocol utilizing an economical and versatile catalyst optimising its use exploiting continuous-flow reactor technologies. We directed our attention to Octahedral Molecular Sieves (OMS),²² that are cryptomelane-structured manganese-based catalysts that possess unique properties such as 1D tunnel structures with tuneable angstrom-scale dimensions, mixed valent Mn ions assembled in an octahedral chain to form a cavity that can allocate different cations. Importantly, OMS have a high lattice oxygen mobility that renders this catalyst highly stable and excellent for oxidation reactions.²³

Some preliminary data are available on the oxidation of HMF to DFF with OMS. At the same time,²⁴ surprisingly, there have been very limited reports on the catalytic oxidation of HMF to FDCA using OMS-based catalysts.²⁵

In a previous study, we demonstrated that OMS-2 catalyst can be utilised in flow in the presence of a gaseous reagent with excellent performances in terms of catalyst oxidation state and leaching stability.²⁶ Herein, also considering the many challenges listed above, we reasonably envisaged that adopting continuous-flow conditions could be helpful to decrease the hazard associated with the use of gaseous oxygen or air with a concomitant increase in control of the reaction parameters that are critical to reduce byproduct formation and increase the yield of FDCA.

Considering all these aspects, we present herein our study on the definition of a sustainable flow process for the oxidation of HMF to FDCA. The concomitant use of a synthetically simple Mn-based catalyst (OMS) and air as an oxidant was made possible by the implementation of a continuous flow system based on tube-in-tube technology. In this way, the manganese catalyst proved to be an interesting system in terms of performance and temperature of use with catalysts based on noble metals. The combination of a well-defined (octahedral) catalytic cavity with a tuneable acidity microenvironment proved to be beneficial for the catalytic oxidation of HMF to FDCA (Fig. 1).

Results and discussion

After preparing and characterising the K-OMS-2 catalyst,^{26,27} we began our study by optimising the reaction conditions for the selective oxidation of HMF to FDCA in a batch reactor.



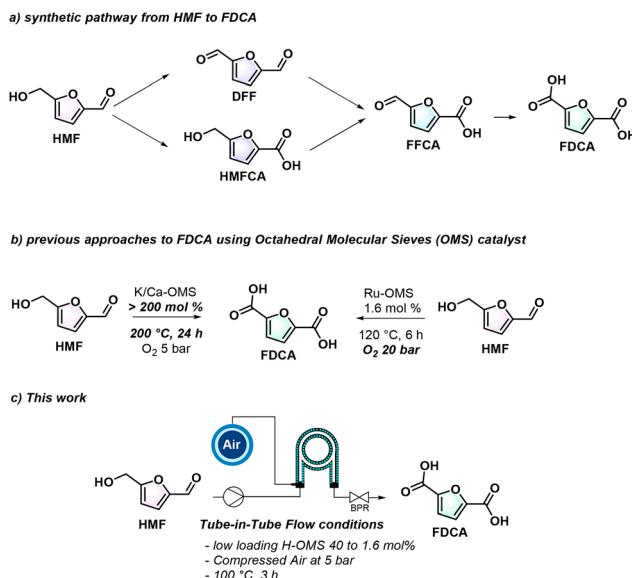


Fig. 1 Features of the previous report and this work.

By fixing the catalyst loading at a 20% molar ratio compared to the HMF starting material (Mn content in K-OMS-2 catalyst is 62%), we tested the influence of different inorganic bases, temperatures and oxygen pressure on the conversion and selectivity of the process (Table 1). As humins are difficult to reveal by common UV-HPLC coupled techniques and, in

Table 1 Optimisation of reaction conditions for the selective oxidation of **1** to **2**^a

Entry	Base	T (°C)	O ₂ (bar)	K-OMS-2 (20 mol %)	
				Base, O ₂	Water (20 mL), T (°C), 24 h
1	NaOH	120	10	>99	95
2	NaHCO ₃	120	10	>99	95
3	NaOH	120	10	87	72
4	NaHCO ₃	120	10	82	70
5	KOH	120	10	>99	84
6	K ₂ CO ₃	120	10	>99	68
7	Na ₂ CO ₃	120	10	>99	78
8	Cs ₂ CO ₃	120	10	>99	76
9	NaOH	100	10	94	71
10	NaOH	80	15	62	78
11	NaOH	120	5	75	61
12	NaHCO ₃	100	10	93	73
13	NaHCO ₃	80	15	54	73
14	NaHCO ₃	120	5	77	62
15	NaHCO ₃	150	5	98	62
16	NaHCO ₃	120	— ^c	8	—

^a Reaction conditions: HMF **1** (1 mmol), in 20 mL of 0.1 M water solution of the selected base, base (2 eq.), K-OMS-2 catalyst (20 mol%, 18 mg). ^b Conversion and selectivity, were determined by HPLC analysis, the remaining material, unless otherwise stated is a mixture of DFF, HMFC, FFCA and unreacted HMF **1**. ^c N₂ at a pressure of 5 bar was used.

most cases, cannot be measured concomitantly with the other reaction products, quantitative calibration curves have been performed to check whether the formation of humins could affect the mass balance and also leading to partially wrong interpretations. We considered this as an important parameter to control and ultimately achieve the isolation of FDCA in high yield and purity. The most performant reaction conditions were exploited either when two equivalents of NaHCO₃ or NaOH were used as a base at 120 °C in the presence of 10 bar of pure oxygen for 24 h (Table 1, entries 1 and 2). In these conditions, HMF has been almost fully and selectively converted to FDCA with a very minimal amount (5%) of FFCA as an incomplete oxidation byproduct. It is worth noting that this result is in line with experimental results obtained from literature protocols using similar catalysts and conditions.

Further optimisation has been aimed at checking whether the changes in the acid/base properties of the catalyst could affect the outcomes of the reaction. To this end, the H-OMS-2 catalyst has been prepared^{26,27} and used instead of K-OMS-2. By replacing K⁺ cation with H⁺ in the tunnel's cavity, a progressive increase in acidity of these sites is induced,²⁸ and therefore an overall increase in Brønsted acidity of the catalyst while maintaining almost unchanged the percentage of manganese content. This type of acidic site has been found to be crucial in controlling oxygen mobility, also influencing the oxidation of HMF to its intermediates and ultimately to FDCA.^{18a,b,29} In addition, to smoothen the operations in terms of safety and avoiding the use of high-pressure gases (pressurised cylinders), but also to avoid the use pure oxygen, we also screened the use of air from a compressor at different pressures (Table 2).

Table 2 Optimisation of reaction conditions for the selective oxidation of **1** to **2**^a

Entry	Catalyst	Oxidant gas (bar)	cat 20 mol % NaHCO ₃ , O ₂	
			Water (20 mL), 120 °C, 24 h	2
1	H-OMS-2	Oxygen (10)	>99	98
2	K-OMS-2	Oxygen (8)	>99	95
3	H-OMS-2	Oxygen (8)	>99	98
4	K-OMS-2	Oxygen (4)	95	90
5	H-OMS-2	Oxygen (4)	>99	98
6	K-OMS-2	Oxygen (2)	90	87
7	H-OMS-2	Oxygen (2)	98	98
8	K-OMS-2	Air (2)	55	60
9	H-OMS-2	Air (2)	64	77
10	K-OMS-2	Air (8)	90	85
11	H-OMS-2	Air (8)	95	98
12	K-OMS-2	Air (10)	96	94
13	H-OMS-2	Air (10)	>99	98

^a Reaction conditions: HMF **1** (1 mmol), in 20 mL of 0.1 M water solution of the selected base, base (2 eq.), catalyst 20 mol%. ^b Conversion and selectivity, were determined by HPLC analysis, the remaining material, unless otherwise stated is a mixture of DFF, HMFC, FFCA and unreacted HMF **1**.

Interestingly, we noted that the catalytic performances of H-OMS were almost identical to those of K-OMS-2. The substantial difference is that H-OMS-2 is more selective than K-OMS-2 at the same oxygen pressure (Table 2, entries 2 to 7), which probably depends on the increased ability of H-OMS-2 (increased Brønsted acidity) to adsorb HMF onto the Mn ions by sharing a lone pair with the -OH group of HMF.

We noted that it is also possible to use air instead of oxygen, either with K-OMS-2 or H-OMS-2 as catalytic systems. Anyway, the pressure must be at least 10 bar to achieve satisfactory conversions and selectivities (Table 2, entries 8 to 13).

We also tested the reusability of the two catalytic systems, H- and K-OMS-2 and data are reported in Table 3. The first attempt was aimed at the identification of suitable conditions to recycle the catalysts efficiently. In the optimised reaction conditions, we noted that 20 mol% of hydrogen peroxide with respect to HMF was crucial in this phase to maintain unchanged the oxidation ability of the two catalysts, with H-OMS-2 possessing slightly better performance compared to K-OMS-2.

Control experiments were made to exclude the possibility that hydrogen peroxide/oxygen could act as an oxidant system in the absence of the catalyst.

As encouraging results were obtained in terms of reactivity, selectivity, catalyst stability, and overall efficiency of the developed system, we also verified the isolation of pure FDCA product. To this end, after the reaction completion, catalyst was filtered (sintered glass, porosity 4–8 µm) and the filtrate was acidified to pH 1. Using H₂SO₄, the precipitation of FDCA from the reaction mixture was very slow (12 h), and the resulting yield was only 83%. Using HCl, the precipitation occurred much faster (6–8 h of maturation), and the yield was 91%.

We found useful the comparison of our optimised conditions with other protocols using OMS-type catalysts for the conversion of HMF either to FDCA or to DFF. For a better

assessment, we also compared our conditions with a very simple yet efficient protocol that uses simple and benchmark MnO₂ as catalyst³⁰ (Table 9).

With this preliminary comparison, we can note that among the other OMS-based methodologies to achieve FDCA from HMF, our optimised conditions allow the use of oxygen or air with comparable efficiency, and among the non-noble Mn-based catalyst, we also use a lower loading (20 mol%) and a lower temperature (120 °C). Notably, selectivity to FDCA (avoiding DFF), is advantageous. With the intention to increase the efficiency of our methodology, we started to evaluate different continuous-flow settings and verify how this can influence the intimacy between sacrificial oxidant (oxygen or air) and the reaction mixture. We designed, built and tested five flow reactor systems (Fig. 2).

Using our previously developed flow conditions²⁶ in which the gas flow drives the reaction mixture through the catalyst reactor (Table S1 in the ESI†), almost no reaction occurred, highlighting how important the delivering of terminal oxidant (O₂) to the reaction mixture. Importantly, very low conversion of HMF was observed with the tested conditions.

Therefore, we changed the continuous-flow reactor setting using a standard T connection (Table 4). With this configuration, no encouraging results were obtained, giving a further confirmation of the importance of the delivering of terminal oxidant. In these conditions, 42% of HMF conversion was anyway observed but with a very poor 15% selectivity toward FDCA (Table 4, entry 1). The remaining material was composed of 18% of DFF and 25% of HMFCA. With this system, decreasing the temperature from 120 to 100 °C led to a dramatic decrease in conversion (22%) with a 12% selectivity to FDCA (Table 4, entry 2), and DFF as the only remaining material.

We also tested another configuration in which the T connection delivering the oxygen was installed in the middle of the packed bed reactor (Table 5).

The resistance of the flowing reaction mixture against the oxygen counterpressure should, in principle, increase the oxygenation of the whole mixture, increasing the efficiency. In fact, with this configuration we observed a 24% selectivity toward FDCA (Table 5, entry 1) which lowered to 20% (Table 5, entry 4) when the oxygen pressure is decreased to 5 bar. We also noted that a valuable influence is attributed to an increase

Table 3 Recyclability of OMS catalysts^a

Entry	Catalyst	Additive	1 st run C/Sel ^b (%)	2 nd run C/Sel ^b (%)
1	H-OMS-2	None	>99/98	>99/89
2	K-OMS-2	None	>99/95	>99/85
3 ^c	H-OMS-2	H ₂ O ₂	>99/98	>99/92
4 ^c	K-OMS-2	H ₂ O ₂	>99/95	>99/91
5 ^d	H-OMS-2	H ₂ O ₂	>99/98	>99/98
6 ^d	K-OMS-2	H ₂ O ₂	>99/95	>99/93
7	None	H ₂ O ₂	12/—	—

^a Reaction conditions: HMF **1** (1 mmol), in 20 mL of 0.1 M water solution of the selected base, base (2 eq.), catalyst 20 mol%. ^b Conversion and selectivity, were determined by HPLC analysis, the remaining material, unless otherwise stated is a mixture of DFF, HMFCA, FFCA and unreacted HMF **1**. ^c H₂O₂ 5 mol% respect to HMF was used as additive. ^d H₂O₂ 20 mol% respect to HMF was used as additive.

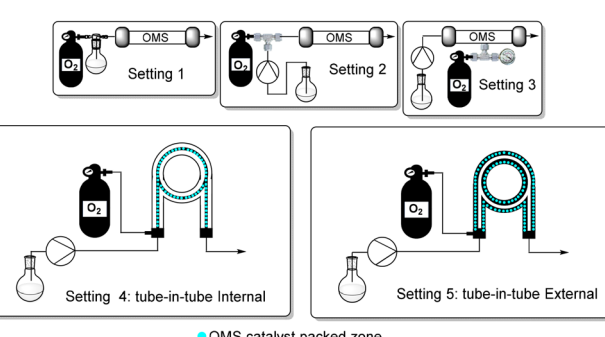


Fig. 2 Flow configurations tested.

Table 4 Oxidation of HMF to FDCA using a *T* connection to supply oxygen (setting 2)^a

Entry	O ₂ (bar)	T (°C)	Residence time (h)	HMF C ^b (%)	FDCA Sel ^b (%)
1	10	120	3	42	15
2	10	100	3	22	12
3	10	100	2	0	—
4	5	120	3	0	—
5	5	100	3	0	—
6	5	100	2	0	—
7	2	120	3	0	—
8	1	120	3	0	—
9	1	120	5	0	—

^a Reaction conditions: **1** (1 mmol), in 20 mL of 0.1 M NaHCO₃ water solution. Flow reactor parameters: length of the packed bed reactor = 20 cm; internal diameter = 0.4 cm; catalyst loaded = 90 mg (100 mol%). ^b Conversion and selectivity, were determined by HPLC analysis, the remaining material, unless otherwise stated, is a mixture of DFF, HMFCA, FFCA and unreacted HMF **1**.

Table 5 Oxidation of HMF to FDCA with middle oxygen delivery (setting 3)^a

Entry	O ₂ (bar)	T (°C)	Residence time (h)	HMF C ^b (%)	FDCA Sel ^b (%)
1	10	120	3	58	24
2	10	100	3	44	20
3	10	100	2	38	18
4	5	120	3	35	20
5	5	100	3	30	20
6	5	100	2	18	15
7	2	120	3	0	—
8	1	120	3	0	—
9	1	120	5	0	—

^a Reaction conditions: **1** (1 mmol), in 20 mL of 0.1 M NaHCO₃ water solution. Flow reactor parameters: length of the packed bed reactor = 20 cm; internal diameter = 0.4 cm; catalyst loaded = 90 mg (100 mol%). ^b Conversion and selectivity, were determined by HPLC analysis, the remaining material, unless otherwise stated, is a mixture of DFF, HMFCA, FFCA and unreacted HMF **1**.

in residence time (from 2 h to 3 h) rather than to the oxygen pressure or temperature set (Table 5, entries 2, 3 and 5, 6). On the other hand, at oxygen pressure as low as 2 or 1 bar, HMF did not react efficiently.

We decided to utilise our newly developed heterogeneous tube-in-tube reactor,³¹ which, differently from all the pre-

Table 6 Oxidation of HMF to FDCA using tube-in-tube technology (setting 4)^a

Entry	O ₂ (bar)	T (°C)	Residence time (h)	HMF C ^b (%)	FDCA Sel ^b (%)
1	10	120	3	84	69
2	10	100	3	76	72
3	10	100	2	65	70
4	5	120	3	60	68
5	5	100	3	54	75
6	5	100	2	48	70
7	2	120	3	34	66
8	1	120	3	30	61
9	1	100	3	24	64
10	1	120	5	38	62

^a Reaction conditions: **1** (1 mmol), in 20 mL of 0.1 M NaHCO₃ water solution. Flow reactor parameters: length of the outer tube (gas reservoir tube) = 20 cm; internal diameter = 0.4 cm; length of the inner tube (AF2400, packed bed) = 20 cm; internal diameter = 0.1 cm; catalyst loaded = 36 mg (40 mol%). ^b Conversion and selectivity, were determined by HPLC analysis, the remaining material, unless otherwise stated, is a mixture of DFF, HMFCA, FFCA and unreacted HMF **1**.

viously developed systems in literature, features the catalyst inside the AF-2400 tube (internal diameter: 0.1 cm), where the reaction mixture flows. Oxygen is flowed in the outer tube (internal diameter 0.4 cm) at the desired pressure. As a result, the contact between HMF, OMS, and O₂ was increased, and we observed a satisfactory conversion of HMF both at 120 and 100 °C with a residence time of 3 h (Table 6, entries 1 and 2).

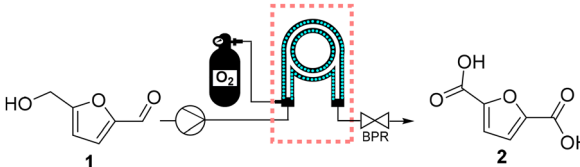
Importantly, we experimented that with this system, HMF can be oxidised even at a very low oxygen pressure (1 bar), furnishing low conversion (30% and 38%, respectively, with 3 and 5 hours of residence time) and acceptable selectivity to FDCA (Table 6, entries 8 and 10).

As in the above-described flow system (setting 4, Table 6), we noted that, especially at low pressure of oxygen, the conversion drops dramatically while the selectivity toward FDCA remains almost constant. Therefore, we designed another configuration (setting 5, Table 7) of the tube-in-tube flow system where the catalyst is packed in the outer tube (internal diameter 0.4 cm), and the oxygen pressure-charged at the inner permeable tube (internal diameter 0.1 cm). In our view, this configuration could increase the contact surface between catalyst and reaction mixture, maintaining constant the efficiency of the oxygen supply.

With reactor setting 5, the conversion of HMF at 5 bar of pressure is complete both at 120 and at 100 °C with full selectivity to FDCA (Table 7, entries 4–6). Decreasing the oxygen pressure to 1 bar slightly decreases the conversion while the selectivity remains high (Table 7, entries 8 and 9).

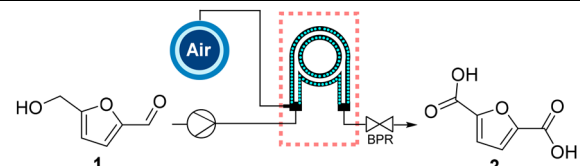
Finally, we tested the performance of last continuous flow system (setting 5) using air generated with a common compressor (Table 8). We were pleased to note that at 5 bar of



Table 7 Oxidation of HMF to FDCA using tube-in-tube technology (setting 5)^a


Entry	O ₂ (bar)	T (°C)	Residence time (h)	HMF C ^b (%)	FDCA S ^b (%)
1	10	120	3	>99	100
2	10	100	3	>99	100
3	10	100	2	>99	100
4	5	120	3	>99	100
5	5	100	3	>99	100
6	5	100	2	>99	100
7	2	120	3	98	100
8	1	120	3	88	94
9	1	120	5	92	100

^a Reaction conditions: **1** (1 mmol), in 20 mL of 0.1 M NaHCO₃ water solution. Flow reactor parameters: length of the outer tube (packed bed) = 20 cm; internal diameter = 0.4 cm; length of the inner tube (AF2400, gas reservoir) = 20 cm; internal diameter = 0.1 cm; catalyst loaded (at the outer tube) = 36 mg (40 mol%). ^b Conversion and selectivity, were determined by HPLC analysis, the remaining material, unless otherwise stated, is a mixture of DFF, HMFCA, FFCA and unreacted HMF **1**.

Table 8 Oxidation of HMF to FDCA using common tube-in-tube technology with air^a


Entry	Air (bar)	T (°C)	Residence time (h)	HMF C ^b (%)	FDCA S ^b (%)
1	10	120	3	>99	100
2	10	100	3	>99	100
3	10	100	2	>99	100
4	5	120	3	>99	100
5	5	100	3	>99	100
6	5	100	2	95	100
7	2	120	3	83	85
8	1	120	3	60	43
9	1	120	5	67	59
10	2	80	5	35	56
11	5	80	5	41	62

^a Reaction conditions: **1** (1 mmol), in 20 mL of 0.1 M NaHCO₃ water solution. Flow reactor parameters: length of the outer tube (packed bed) = 20 cm; internal diameter = 0.4 cm; length of the inner tube (AF2400, gas reservoir) = 20 cm; internal diameter = 0.1 cm; catalyst loaded (at the outer tube) = 36 mg (40 mol%). ^b Conversion and selectivity, were determined by HPLC analysis, the remaining material, unless otherwise stated, is a mixture of DFF, HMFCA, FFCA and unreacted HMF **1**.

pressure, conversion and selectivity are almost unchanged, passing from pure oxygen to compressed air (non-purified) both at 120 and 100 °C. Lowering the pressure or the temperature, respectively, below 5 bar and 100 °C, led to a progressive and linear decrease in the system's efficiency. Interestingly, the calculation of the average residence time (\bar{r}) for all five flow settings presented allowed us to appreciate that, especially for settings 4 and 5, there was a significant deviation between the effective residence time and the average residence time, denoting a plausible strong variation from ideal flow behaviour due to the non-conventional flow configuration and packing.

The flow system developed was finally stressed to check its productivity and the amount of metal leached in solution, which could negatively affect the overall durability of the system. The flow apparatus was therefore tested in optimised conditions at 100 °C with 5 bar of air pressure. Letting the flow apparatus run continuously for 3 days and checking aliquots of the reaction mixture allowed us to check the presence of metal contaminants and the reactivity limits of the catalyst (Fig. 3).

We noted that after the first half of the first day of continuous flow operation, there was no decrease in efficiency. After 12 hours, we noted a slight decrease in terms of conversion with the selectivity that was kept at excellent levels. During the 2nd and third-day of flowing, the performance remained constant with an average conversion of 98% and 100% selectivity toward FDCA.

Interestingly, we noted that the optimised flow systems does not require the addition of hydrogen peroxide or other co-oxidants to maintain the catalytic performances. This behaviour was also confirmed by the continuous monitoring of the Mn leaching, which constantly remained under 1 ppm.

Also, the isolated yield slightly increased compared to batch conditions (91% in batch vs. 93% in flow), and therefore we obtained a daily production of 7.2 mmol day⁻¹ of FDCA. At the steady state, our flow system was able to produce 0.3 mmol h⁻¹ (48 mg h⁻¹ of FDCA) with a space–time yield of 19.1 g L⁻¹ h⁻¹.

It is worthy to notice that these data have been obtained with a small apparatus containing 36 mg of catalyst only. Sizing appropriately to gram scale catalyst and larger systems the productivity is very promising.

Notably, by adopting our flow conditions, we were able to efficiently and durably use a simple-to-synthesise, low-cost manganese-based catalyst. Above all, under the optimised conditions, the manganese catalyst was used at a relatively low temperature (100 °C) and pressure (5 bar of air), exploiting comparable efficiency to noble metal-based catalysts.

Ultimately, we have compared the results obtained.

The *E*-factor of our flow methodology was calculated together with the *E*-factor of the previously mentioned OMS-based procedures used to synthesise FDCA. Gratefully, we achieved an *E*-factor value as low as 139, which is the lowest among the OMS-based protocols overviewed. The low *E*-factor obtained in our optimised flow procedure is basically due to the high yield of FDCA obtained (93%) and to the



Table 9 Comparison of literature available protocols in batch conditions

Ref. (target)	Catalyst (mg)/loading to HMF (mol %)	T (°C)/time (h)	Solvent [Molarity]	Gas (bar)	Selectivity	Reusability
30 (FDCA)	MnO ₂ (100 mg)/575 mol%	100/24	Water [0.04 M]	O ₂ (10)	91	Yes
25a (FDCA)	K-MnO ₂ (125 mg)/262 mol%	200/24	Water [0.05 M]	O ₂ (5) + air (1)	49	Yes
25a (FDCA)	Ca-MnO ₂ (125 mg)/274 mol%	200/24	Water [0.05 M]	O ₂ (5) + air (1)	85	Yes
25b (FDCA)	Ru-K-OMS-2 (80 mg)/1.6 mol% ^a	120/6	Water [0.05 M]	O ₂ (20)	93	n.t.
24a (DFF)	Ag-OMS-2 (300 mg)/16 mol%	200/4–6	IPA [0.06 M]	Air (15)	100	Yes
24b (DFF)	K-OMS (60 mg)/65 mol%	120/10	DMSO [0.2 M]	O ₂ (1)	100	Yes
24c (DFF)	K-OMS-2 (22 mg)/22 mol%	110/1	DMF [0.1 M]	O ₂ (5)	97	Yes
24d (DFF)	K-OMS-2 (100 mg)/101 mol%	110/6	DMSO [0.3 M]	O ₂ (20)	99	Yes
This work (FDCA)	H-OMS-2 (18 mg)/20 mol%	120/24	Water [0.05 M]	Air (10) or O ₂ (4)	98	Yes

^a 1.6 mol% is the loading of ruthenium catalyst compared to HMF (with Ru is 2% in Ru-K-OMS-2), while must also be considered that an average 60% is Mn whose loading will be 87 mol% compared to HMF; n.t. means non tested for recyclability.

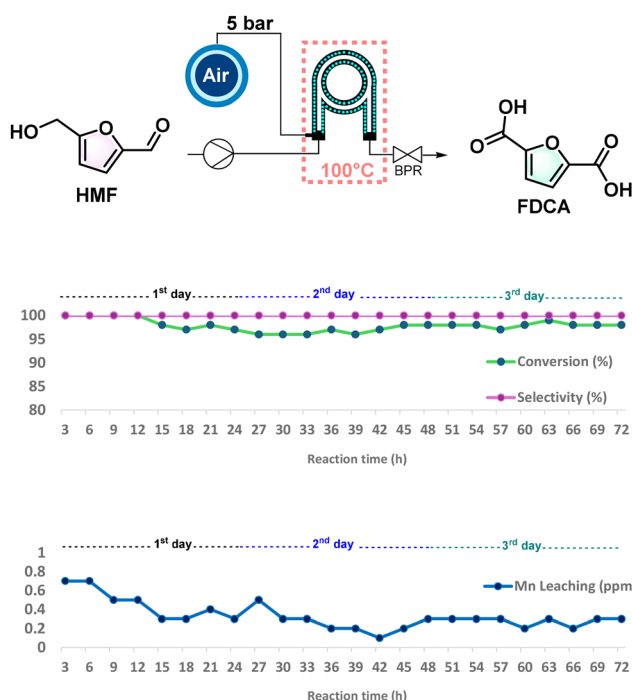


Fig. 3 Conversion, selectivity and leaching profile of the 3 day flow session.

amount of base used (2 equivalents *vs.* at least 3 equivalents of the other protocols), which smooth the isolation procedure of FDCA.

Further quantification of the advantages of our flow methodology was based on the calculation of STY, which, not surprisingly, has a better value than the other processes as a consequence of the adoption of flow conditions within good throughput (48 mg h⁻¹ of FDCA) in a small volume of the reactor (2.5 mL) with a relatively short residence time (3 h).

By calculating reaction temperature and pressure Hazard Indexes (respectively RTHI and RPHI) with Andraos algorithms, we could also quantify the hazard associated with temperature or pressure different from ambient conditions usage, with RTHI and RPHI that vary between 0 and 1 (1 is a benign situation while 0 is an extremely hazardous situation, see ESI† for detailed calculations). Importantly, our flow procedure allowed us to reduce the hazard associated with the pressure of reaction, leading to the best RPHI value among the procedures compared, while RTHI values are by far equal to the MnO₂ benchmark procedure.

To quantify more in details the utility of using our flow apparatus based on tube-in-tube technology, in terms of yield (conversion and selectivity towards FDCA), short times and at relatively low temperatures and pressure (100 °C

Table 10 Sustainability comparison for the synthesis of FDCA using Mn-based and OMS catalyst

Ref.	Features	T (°C)	RTHI	Gas (bar)	RPHI	E-factor with H ₂ O/without H ₂ O	STY (g L ⁻¹ h ⁻¹)	Oxygen efficiency
30	MnO ₂ (0.2 mmol)	100	0.78	O ₂ (10)	0.00014	1765/5.2	0.09	8.4%
30	MnO ₂ (18 mmol)	100	0.78	O ₂ (10)	0.00014	193/138	0.35	26.7%
25a	K-OMS (0.25 mmol)	200	0.56	O ₂ (5) + air (1)	0.0073	734/211	0.04	5.7%
25a	Ca-OMS (0.25 mmol)	200	0.56	O ₂ (5) + air (1)	0.0073	423/121	0.07	10.0%
25b	Ru-OMS (1 mmol)	120	0.72	O ₂ (20)	0.0000000072	No isolation	0.48	5.8%
This work	H-OMS (1 to 24 mmol)	100	0.78	Air (5)	0.020	139/1.2	19.1	45.7%



and 5 bar of air), we considered the oxygen efficiency (see ESI[†] for details) as:

$$\frac{\text{O}_2\text{-equiv.}}{\text{Mol oxygen}} \times 100$$

$$\frac{\text{Mol product}}{\text{Mol oxygen}}$$

$\text{O}_2\text{-equiv.}$ is the stoichiometric amount of molecular oxygen needed in the reaction. From the results of the oxygen efficiency calculations (Table 10), it is worthy to notice that the use of tube-in-tube flow technology allowed us to reach the optimal oxygen efficiency of 45.7%, while for all the other processes compared, it is below 26.7%.

Conclusions

In conclusion, in this work, we demonstrated that, within a stepwise optimisation of reaction conditions and technological flow set-up, a simple yet efficient Mn-based octahedral molecular sieves catalyst (H-OMS-2) could achieve similar or even better performance compared to the noble metal-based catalyst of the same type (OMS), in the selective oxidation of HMF to FDCA. Tube-in-tube flow conditions, in combination with the Mn-based heterogeneous catalyst, allowed the utilisation of air at a relatively low pressure of 5 bar. The flow system developed was efficiently used to synthesise FDCA in high yield (93%) with an STY of $19.1 \text{ g L}^{-1} \text{ h}^{-1}$ and productivity of 48 mg h^{-1} . The 3 day flow session was exploited with excellent performance in terms of conversion, selectivity, and stability (Mn leaching).

To confirm the overall value of our protocol in terms of sustainability, we compared it with other procedures in the literature for the *E*-factor, hazard associated with temperature and pressure usage, and oxygen efficiency. Our tube-in-tube flow conditions exploiting air at 5 bar of pressure led to optimal values of oxygen efficiency and *E*-factor with considerable risk reduction associated with temperature and pressure.

Author contributions

The manuscript was written with contributions from all authors. All authors have approved the final version of the manuscript. F. V: investigation, methodology, data analysis, manuscript preparation – review; F. F.: investigation, methodology, data analysis, manuscript preparation – review; L. V.: conceptualisation, project administration, manuscript review/editing.

Data availability

The data supporting this article have been included as part of the ESI.[†]

Conflicts of interest

There are no conflicts to declare.

Acknowledgements

This work has been funded by the European Union – NextGenerationEU under the Italian Ministry of University and Research (MUR) National Innovation Ecosystem grant ECS00000041 – VITALITY. We acknowledge Università degli Studi di Perugia and MUR for support within the project Vitality. The University of Perugia is acknowledged for financial support to the university project “Fondo Ricerca di Ateneo, edizione 2022”. MUR is also thanked for PRIN-PNRR 2022 project “P2022XKWH7 – CircularWaste”.

References

- 1 (a) R. A. Sheldon, *Green Chem.*, 2014, **16**, 950–963; (b) A. Corma, S. Iborra and A. Velty, *Chem. Rev.*, 2007, **107**, 2411–2502; (c) H. Kobayashi and A. Fukuoka, *Green Chem.*, 2013, **15**, 1740–1763; (d) P. Gallezot, *Chem. Soc. Rev.*, 2012, **41**, 1538–1558; (e) J. J. Bozell and G. R. Petersen, *Green Chem.*, 2010, **12**, 539–554.
- 2 (a) R. A. Sheldon and D. Brady, *ChemSusChem*, 2019, **12**, 2859–2881; (b) J. B. Zimmerman, P. T. Anastas, H. C. Erythropel and W. Leitner, *Science*, 2020, **367**, 39; (c) N. Armaroli and V. Balzani, *Angew. Chem., Int. Ed.*, 2007, **46**, 52–66.
- 3 (a) C. Rossi, L. Shen, M. Junginger and B. Wicke, *J. Cleaner Prod.*, 2024, **468**, 143079Y; (b) P. Morone, R. Caferra, I. D'Adamo, P. M. Falcone, E. Imbert and A. Morone, *Int. J. Prod. Econ.*, 2021, **240**, 108248.
- 4 (a) S. Y. Lee, H. U. Kim, T. U. Chae, J. S. Cho, J. W. Kim, J. H. Shin, D. I. Kim, Y.-S. Ko, W. D. Jang and Y.-S. Jang, *Nat. Catal.*, 2019, **2**, 18–33; (b) L. R. Lynd, G. T. Beckham, A. M. Guss, L. N. Jayakody, E. M. Karp, C. Maranas, R. L. McCormick, D. Amador-Noguez, Y. J. Bomble, B. H. Davison, C. Foster, M. E. Himmel, E. K. Holwerda, M. S. Laser, C. Y. Ng, D. G. Olson, Y. Román-Leshkov, C. T. Trinh, G. A. Tuskan, V. Upadhayay, D. R. Vardon, L. Wang and C. E. Wyman, *Energy Environ. Sci.*, 2022, **15**, 938–990.
- 5 (a) B. Jacobs, Y. W. Yao, I. Van Nieuwenhove, D. Sharma, G. J. Graulus, K. Bernaerts and A. Verberckmoes, *Green Chem.*, 2023, **25**, 2042–2086; (b) R. Hu, J. Zhan, Y. Zhao, X. Xu, G. Luo, J. Fan, J. H. Clark and S. Zhang, *Green Chem.*, 2023, **25**, 8970–9000; (c) J. H. Clark, V. Budarin, F. E. I. Deswarde, J. J. E. Hardy, F. M. Kerton, A. J. Hunt, R. Luque, D. J. Macquarrie, K. Milkowski, A. Rodriguez, O. Samuel, S. J. Tavener, R. J. White and A. J. Wilson, *Green Chem.*, 2006, **8**, 853; (d) J. F. Jenck, F. Agterberg and M. J. Droscher, *Green Chem.*, 2004, **6**, 544–556.



6 (a) J. J. Bozell, *Science*, 2010, **329**, 522–523; (b) J. J. Bozell, *Clean: Soil, Air, Water*, 2008, **36**, 641.

7 (a) B. Y. Karlinskii and V. P. Ananikov, *Chem. Soc. Rev.*, 2023, **52**, 836–862; (b) Z. Jiang, Y. Zeng, D. Hu, R. Guo, K. Yan and R. Luque, *Green Chem.*, 2023, **25**, 871–892; (c) Q. Hou, X. Qi, M. Zhen, H. Qian, Y. Nie, C. Bai, S. Zhang, X. Bai and M. Ju, *Green Chem.*, 2021, **23**, 119–231; (d) C. Xu, E. Paone, D. Rodríguez-Padrón, R. Luque and F. Mauriello, *Chem. Soc. Rev.*, 2020, **49**, 4273–4306.

8 (a) N. Guigo, F. Jérôme and A. F. Sousa, *Green Chem.*, 2021, **23**, 9721–9722; (b) R.-J. van Putten, J. C. van der Waal, E. de Jong, C. B. Rasrendra, H. J. Heeres and J. G. de Vries, *Chem. Rev.*, 2013, **113**, 1499–1597; (c) S. P. Teong, G. Yi and Y. Zhang, *Green Chem.*, 2014, **16**, 2015–2026; (d) T. Werpy and G. Petersen, *Top value-added chemicals from biomass: volume I-results of screening for potential candidates from sugars and synthesis gas*, National Renewable Energy Lab., Golden, CO., US, 2004.

9 (a) M. Khalid, M. Granollers Mesa, D. Scapens and A. Osatiashtiani, *ACS Sustainable Chem. Eng.*, 2024, **12**, 16494–16517; (b) M. Sajid, U. Farooq, G. Bary, M. M. Azim and X. Zhao, *Green Chem.*, 2021, **23**, 9198–9238; (c) Z. Zhang, *ChemSusChem*, 2016, **9**, 156–171; (d) F. D. Pileidis and M.-M. Titirici, *ChemSusChem*, 2016, **9**, 562–582.

10 (a) D. J. Aranha and P. R. Gogate, *Ind. Eng. Chem. Res.*, 2023, **62**, 3053; (b) G. Totaro, L. Sisti, P. Marchese, M. Colonna, A. Romano, C. Gioia, M. Vannini and A. Celli, *ChemSusChem*, 2022, **15**, e20220050; (c) M. Sajid, X. Zhao and D. Liu, *Green Chem.*, 2018, **20**, 5427–5453; (d) Z. Zhang and G. W. Huber, *Chem. Soc. Rev.*, 2018, **47**, 1351–1390; (e) Z. Zhang and K. Deng, *ACS Catal.*, 2015, **5**, 6529–6544; (f) S. Hameed, W. Liu, Z. Yu, J. Pang, W. Luo and A. Wang, *Green Chem.*, 2024, **26**, 7806–7817.

11 (a) R. M. Cywar, N. A. Rorrer, C. B. Hoyt, G. T. Beckham and E. Y.-X. Chen, *Nat. Rev. Mater.*, 2022, **7**, 83–103; (b) R. A. Sheldon and M. Norton, *Green Chem.*, 2020, **22**, 6310–6322; (c) S. Spierling, E. Knüpfffer, H. Behnson, M. Mudersbach, H. Krieg, S. Springer, S. Albrecht, C. Herrmann and H. J. Endres, *J. Cleaner Prod.*, 2018, **185**, 476e491; (d) A. J. J. E. Eerhart, A. P. C. Faaij and M. K. Patel, *Energy Environ. Sci.*, 2012, **5**, 6407–6422.

12 M. Annatelli, J. E. Sánchez-Velandia, G. Mazzi, S. V. Pandeirada, D. Giannakoudakis, S. Rautiainen, A. Esposito, S. Thiagarajan, A. Richel, K. S. Triantafyllidis, T. Robert, N. Guigo, A. F. Sousa, E. García-Verdugo and F. Aricò, *Green Chem.*, 2024, **26**, 8894–8941, and references cited herein..

13 (a) C. Chen, L. Wang, B. Zhu, Z. Zhou, S. I. El-Hout, J. Yang and J. Zhang, *J. Energy Chem.*, 2021, **54**, 528–554; (b) S. Chen, X. Guo, H. Ban, T. Pan, L. Zheng, Y. Cheng, L. Wang and X. Li, *Ind. Eng. Chem. Res.*, 2021, **60**, 16887–16898; (c) Y. Yao and G. Wang, *J. Phys. Chem. C*, 2021, **125**, 3818–3826.

14 For some recent conventional and unconventional process see: (a) T. Shen, L. Hou, J. Gosset, H. Wang, S. Leng, Y. Boumghar, S. Barghi and C. Xu, *Chem. Eng. J.*, 2024, **500**, 156470; (b) M. A. Do Nascimento, B. Haber, M. R. B. P. Gomez, R. A. C. Leão, M. Pietrowski, M. Zieliński, R. O. M. A. De Souza, R. Wojcieszak and I. Itabaiana Junior, *Green Chem.*, 2024, **26**, 8211–8219; (c) Y. Zhang, G. Jia, W. Wang, L. Jiang and Z. Guo, *Green Chem.*, 2024, **26**, 2949; (d) C. S. Lecona-Vargas and M.-J. Dumont, *Ind. Eng. Chem. Res.*, 2024, **63**, 16222–16246; (e) X. Jiang, X. Ma, Y. Liu, L. Zhao, Y. Zhang, B.-Q. Li and Q. Zhang, *Appl. Catal. B: Environ. Energy*, 2024, **347**, 123785; (f) X. Jiang, W. Li, Y. Liu, L. Zhao, Z. Chen, L. Zhang, Y. Zhang and S. Yun, *SusMat*, 2023, **3**, 21–43; (g) M. G. Davidson, S. Elgie, S. Parsons and T. J. Young, *Green Chem.*, 2021, **23**, 3154–3171; (h) Y. Yang and T. Mu, *Green Chem.*, 2021, **23**, 4228–4254; (i) F. Liguori, P. Barbaro and N. Calisi, *ChemSusChem*, 2019, **12**, 2558–2563; (j) T. Ji, C. Liu, X. Lu and J. Zhu, *ACS Sustainable Chem. Eng.*, 2018, **6**, 11493–11501; (k) J. M. R. Gallo, D. M. Alonso, M. A. Mellmer and J. A. Dumesic, *Green Chem.*, 2013, **15**, 85–90.

15 (a) C. Chen, M. Lv, H. Hu, L. Huai, B. Zhu, S. Fan, Q. Wang and J. Zhang, *Adv. Mater.*, 2024, 2311464R; (b) Y. Wang, H. Wang, X. Kong and Y. Zhu, *ChemSusChem*, 2022, **15**, e202200421; (c) R. Bielski and G. Grynkiewicz, *Green Chem.*, 2021, **23**, 7458–7487.

16 (a) S. Liu, Y. Zhu, Y. Liao, H. Wang, Q. Liu, L. Ma and C. Wang, *Appl. Energy Combust. Sci.*, 2022, 100062; (b) T. M. C. Hoang, E. R. H. Van Eck, W. P. Bula, J. G. E. Gardeniers, L. Lefferts and K. Seshan, *Green Chem.*, 2015, **17**, 959–972; (c) R. Weingarten, J. Cho, R. Xing, W. C. Conner and G. W. Huber, *ChemSusChem*, 2012, **5**, 1280–1290.

17 (a) Y. A. Wei, J. M. Pan, X. Yan, Y. L. Mao and Y. L. Zhang, *ChemSusChem*, 2024, **17**, e202400241; (b) J. Li, G. Wang, X. Wang, Y. Zhao, Y. Zhao, W. Sui, D. Wang and C. Si, *ACS Catal.*, 2024, **14**(21), 16003–16013; (c) H. Liu, X. Tang, X. Zeng, Y. Sun, X. Ke, T. Li, J. Zhang and L. Li, *Green Energy Environ.*, 2022, **7**, 900–932; (d) H. Xu, X. Li, W. Hu, Z. Yu, H. Zhou, Y. Zhu, L. Lu and C. Si, *ChemSusChem*, 2022, **15**, e2022003; (e) P. V. Rathod and V. H. Jadhav, *ACS Sustainable Chem. Eng.*, 2018, **6**, 5766–5771.

18 (a) T. Gao, Y. Yin, G. Zhu, Q. Cao and W. Fang, *Catal. Today*, 2020, **355**, 252–262; (b) D. K. Mishra, H. J. Lee, J. Kim, H.-S. Lee, J. K. Cho, Y.-W. Suh, Y. Yi and Y. J. Kim, *Green Chem.*, 2017, **19**, 1619–1623; (c) J. Deng, H.-J. Song, M.-S. Cui, Y.-P. Du and Y. Fu, *ChemSusChem*, 2014, **7**, 3334–3340.

19 (a) L. Filiciotto, A. M. Balu, J. C. van der Waal and R. Luque, *Catal. Today*, 2018, **302**, 2–15; (b) K. Tashiro, M. Kobayashi, K. Nakajima and T. Taketsugu, *RSC Adv.*, 2023, **13**, 16293–16299; (c) W. Sailer-Kronlachner, C. Rosenfeld, S. Böhmdorfer, M. Bacher, J. Konnerth, T. Rosenau, A. Potthast, A. Geyer and H. W. G. van Herwijnen, *Biomass Convers. Biorefin.*, 2022, **14**, 8711–8728.

20 (a) Y.-T. Huang, J.-J. Wong, C.-J. Huang, C.-L. Li and G.-W. B. Jang, *2,5-Furandicarboxylic Acid Synthesis and Use*, in



Chemicals and Fuels from Bio-Based Building Blocks, Wiley-VCH Verlag GmbH & Co. KGaA, 2016, pp. 191–216. And references cited herein. ; (b) J. N. Chheda, G. W. Huber and J. A. Dumesic, *Angew. Chem., Int. Ed.*, 2007, **46**, 7164–7183 and references cited herein. (c) S. Das, G. Cibin and R. I. Walton, *ACS Sustainable Chem. Eng.*, 2024, **12**, 5575–5585 and references cited herein.

21 For some very recent examples see: (a) F. Ferlin, F. Valentini, F. Campana and L. Vaccaro, *Green Chem.*, 2024, **26**, 6625–6633; (b) F. Valentini, B. Di Erasmo, M. Ciani, S. Chen, Y. Gu and L. Vaccaro, *Green Chem.*, 2024, **26**, 4871–4879; (c) A. N. Khodadadi, E. Cela, D. Marchionni, F. Huang, F. Ferlin and L. Vaccaro, *Green Chem.*, 2024, **26**, 7059–7066; (d) G. Brufani, S. Chen, B. Di Erasmo, A. Afanasenko, Y. Gu, C.-J. Li and L. Vaccaro, *ACS Sustainable Chem. Eng.*, 2024, **12**, 8562–8572; (e) G. Brufani, F. Valentini, G. Rossini, L. Carpisassi, D. Lanari and L. Vaccaro, *Green Chem.*, 2023, **25**, 2438–2445.

22 (a) C. K. King'ondu, N. Opembe, C.-h. Chen, K. Ngala, H. Huang, A. Iyer, H. F. Garcés and S. L. Suib, *Adv. Funct. Mater.*, 2011, **21**, 312–323; (b) S. L. Suib, *Acc. Chem. Res.*, 2008, **41**, 479–487; (c) Y. C. Son, V. D. Makwana, A. R. Howell and S. L. Suib, *Angew. Chem., Int. Ed.*, 2001, **40**, 4280–4283.

23 (a) H. Deng, Y. Lu, T. Pan, L. Wang, C. Zhang and H. He, *Appl. Catal., B*, 2023, **320**, 121955; (b) X. Bi, T. Tang, X. Meng, M. Gou, X. Liu and P. Zhao, *Catal. Sci. Technol.*, 2020, **10**, 360–371; (c) F. Sabaté and M. J. Sabater, *Catalysts*, 2021, **11**, 1147.

24 (a) G. D. Yadav and R. V. Sharma, *Appl. Catal., B*, 2014, **147**, 293–301; (b) B. Sarmah and R. Srivastava, *Mol. Catal.*, 2019, **462**, 92–103; (c) J. Nie and H. Liu, *J. Catal.*, 2014, **316**, 57–66; (d) Z.-Z. Yang, J. Deng, T. Pan, Q.-X. Guo and Y. Fu, *Green Chem.*, 2012, **14**, 2986–2989.

25 (a) T. Poonsawat, P. Promcharoen, T. Meechai, L. C. Chuaitammakit and E. Somsook, *ACS Omega*, 2023, **8**, 47846–47855; (b) N. Lucas, N. R. Kanna, A. S. Nagpure, G. Kokate and S. Chilukuri, *J. Chem. Sci.*, 2014, **126**, 403–413.

26 (a) F. Ferlin, P. M. L. Navarro, Y. Gu, D. Lanari and L. Vaccaro, *Green Chem.*, 2020, **22**, 397–403; (b) F. Ferlin, M. K. Van der Hulst, S. Santoro, D. Lanari and L. Vaccaro, *Green Chem.*, 2019, **21**, 5298–5305.

27 F. Ferlin, A. Marini, N. Ascani, L. Ackermann, D. Lanari and L. Vaccaro, *ChemCatChem*, 2020, **12**, 449–454.

28 R. Kumar, S. Sithambaram and S. L. Suib, *J. Catal.*, 2009, **262**, 304–313.

29 J. Li, R. Wang and J. Hao, *J. Phys. Chem. C*, 2010, **114**, 10544.

30 E. Hayashi, T. Komanoya, K. Kamata and M. Hara, *ChemSusChem*, 2017, **10**, 654–658.

31 F. Ferlin, I. Anastasiou, L. Carpisassi and L. Vaccaro, *Green Chem.*, 2021, **23**, 6576–6582.

